

## Direct imaging of the two-dimensional Fermi contour: Fourier-transform STM

L. Petersen

*Institute of Physics and Astronomy and Center for Atomic-Scale Materials Physics, University of Aarhus, DK 8000 Aarhus C, Denmark*

P. T. Sprunger

*Institute of Physics and Astronomy and Center for Atomic-Scale Materials Physics, University of Aarhus, DK 8000 Aarhus C, Denmark  
and Center for Advanced Microstructures and Devices, Louisiana State University, Baton Rouge, Louisiana 70803*

Ph. Hofmann\*

*Department of Physics and Astronomy, The University of Tennessee, Knoxville, Tennessee 37996-1200  
and Solid State Division, Oak Ridge National Laboratory, Oak Ridge, Tennessee 37831-6057*

E. Lægsgaard

*Institute of Physics and Astronomy and Center for Atomic-Scale Materials Physics, University of Aarhus, DK 8000 Aarhus C, Denmark*

B. G. Briner, M. Doering, H.-P. Rust, and A. M. Bradshaw

*Fritz-Haber-Institut der Max-Planck-Gesellschaft, Faradayweg 4-6, 14195 Berlin, Germany*

F. Besenbacher

*Institute of Physics and Astronomy and Center for Atomic-Scale Materials Physics, University of Aarhus, DK 8000 Aarhus C, Denmark*

E. W. Plummer

*Department of Physics and Astronomy, The University of Tennessee, Knoxville, Tennessee 37996-1200  
and Solid State Division, Oak Ridge National Laboratory, Oak Ridge, Tennessee 37831-6057*

(Received 10 December 1997)

Direct images of the two-dimensional Fermi contour at a surface can be generated by a Fourier transform (FT) of scanning tunneling microscopy (STM) images taken at low-bias voltages. The origins of the Fermi contour in the FT are the standing waves of electrons near the Fermi energy caused by defects in the surface. Several examples of FT-STM are presented to illustrate the simplicity of this technique. The advantages and limitations of this Fermi contour imaging technique are discussed. [S0163-1829(98)51612-8]

The Fermi surface of a metal is in many ways the epitome of quantum solid-state physics. Its shape is dictated by quantum mechanics, Fermi statistics for electrons, and the character of the Bloch states in the solid. Almost every physical observable is related in one way or another to the shape of the Fermi surface. Due to an enhanced propensity for electronic instabilities, Fermiology related issues are even more important in reduced dimensionality than three dimensions.<sup>1</sup> For example, Fermi contour (FC) nesting facilitated in two dimensions can lead to the stabilization of charge-density waves, Kohn anomalies in the phonon dispersion, and a Peierls distortion of the lattice. Although the measurement of the bulk Fermi surfaces has primarily relied on the *de Haas-van Alphen* effect, the technique of choice for surfaces or other two-dimensional (2D) systems has been angle-resolved photoemission spectroscopy (ARPES).<sup>2</sup> More recently, the notoriety of the ARPES technique has extended from its application to high- $T_c$  superconductors.<sup>3</sup> In this paper, we present a different technique for the measurement of the 2D FC, namely, Fourier-transform scanning tunneling microscopy (FT-STM). The technique utilizes the ability of the STM to image oscillations created by surface-state electrons screening defects and steps at surfaces. Since the oscillations are entirely the product of the Fermi-surface singularity in

the electron-hole excitation spectrum, the imaged oscillations reflect the shape of the 2D FC.

Long-range Friedel oscillations<sup>4</sup> surround any impurity in a solid or on the surface of a metal and “screen” the resulting local disturbance. For a point impurity in the bulk these charge oscillations  $\Delta\rho(r)$  have the asymptotic form  $\Delta\rho(r) \propto \cos\{2k_F r + \phi\}/r^3$ , where  $k_F$  is the Fermi wave vector and  $\phi$  is the phase shift associated with the scattering potential. Since the charge density is the square of the wave function, the Friedel wave vector is twice the Fermi wave vector. When the impurity is on a surface that has a well-defined two-dimensional FC, the Friedel oscillations fall off slower, like  $1/r^2$ . Since the STM measures a quantity closely related to the surface local density of states,<sup>5,6</sup> Friedel oscillations in the vicinity of defects are directly observable. Indeed, STM studies of the noble-metal surfaces show wavelike patterns in the vicinity of steps and adatoms.<sup>7,8</sup>

To illustrate the connection between Friedel oscillations and the FC, we begin by reexamining Friedel oscillations on Cu(111).<sup>7,8</sup> Figure 1(a) is a STM image of a Cu(111) acquired at 150 K taken in the constant current mode. To determine the wave vector of the observed Friedel-like charge oscillations, one could fit the waves in the STM image (in selected regions) to a damped sinusoidal function. However,

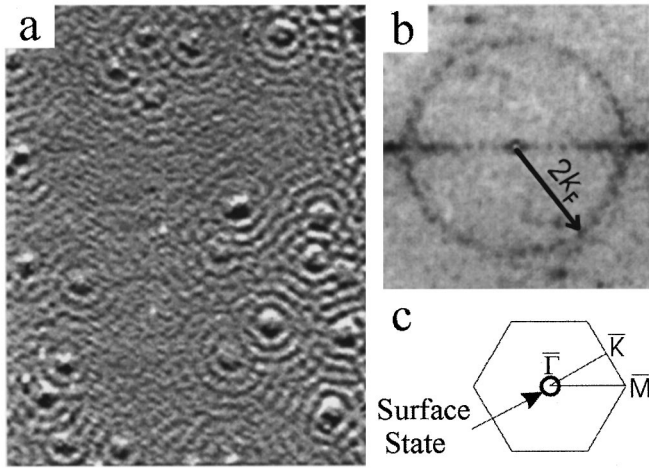


FIG. 1. (a) Constant current STM image ( $425 \times 550 \text{ \AA}^2$ ) of Cu(111) obtained at  $V = -5 \text{ mV}$ ,  $T = 150 \text{ K}$ , showing a complex pattern of circular waves extending out from point defects. (b) 2D Fourier transform of the image in (a). (c) Sketch of the surface Brillouin zone of Cu(111) with the Fermi contour.

a much more elegant method is to Fourier transform the STM image. The 2D power spectrum of Fig. 1(a), shown in Fig. 1(b), reveals that the waves are characterized by a single magnitude wave vector that is azimuthally symmetric about the center. The 2D Brillouin zone of Cu(111) is shown in Fig. 1(c). Previous ARPES studies have determined the Fermi wave vector ( $k_F$ ) of this Shockley-type surface state to be  $0.217 \text{ \AA}^{-1}$ .<sup>9</sup> Within experimental uncertainty, this magnitude is half the radius of the ring measured in the FT-STM image ( $k_F$  vs  $2k_F$  as measured from the ARPES and FT-STM techniques, respectively).

As is readily apparent, this FT-STM technique provides a fast and accurate method of determining the 2D FC, but before proceeding further it is important to discuss the details of the measurement. The STM image shown in Fig. 1(a) was acquired in a low-bias tunneling condition (5 mV), so the observed waves do not reflect true Friedel oscillations, but rather what we refer to as the *energy-resolved* Friedel oscillations, that is, oscillations in the local density of states very near the Fermi level. The importance of this distinction can be illustrated using an exactly solvable model representing a step on a surface. Following the approach of Avouris and co-workers,<sup>8</sup> the step is modeled as a hard wall and the 2D electronic states are represented by a free-electron band with the Fermi wave vector  $k_F$ . In this case the charge density can be determined to be

$$\rho(x) = en_0 \{1 - 2[J_1(2k_F x)] / (2k_F x)\}, \quad (1)$$

where  $J_1$  is the first-order spherical Bessel function and  $n_0$  is the constant 2D electron density of an undisturbed free-electron gas. The dotted curve of Fig. 2(a) shows the calculated charge-density profile from Eq. (1) as a function of the distance  $x$  from the hard wall. This reveals the Friedel oscillations with a wave vector  $q = 2k_F$ , falling off with distance from the step as  $1/x^{3/2}$ . From the FT of Eq. (1), shown as the dotted curve in Fig. 2(b), it is evident that the true Friedel oscillations contain every wave vector from  $k=0$  to  $2k_F$ , with a tail above  $2k_F$  resulting from the power-law depen-

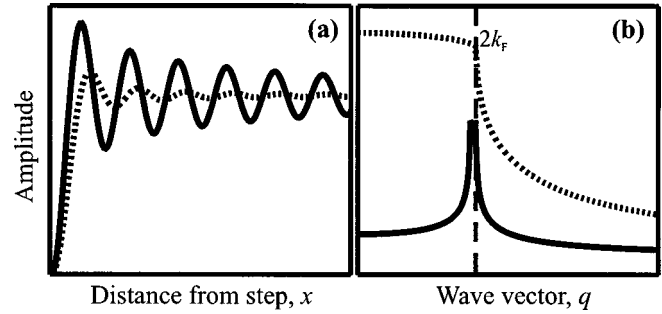


FIG. 2. Induced charge oscillations from a hard wall in 2D. (a) A plot of the calculated induced charge oscillations; dotted (solid) curve is the (energy-resolved) Friedel oscillation represented by Eq. (1) [integration of Eq. (2) over  $0.1 E_F$  energy window]; (b) a plot of the FT of the curves in (a) (solid curve is with bias voltage of  $eV = 0.1 E_F$ ).

dence of the Friedel oscillations. If we had imaged true Friedel oscillations for Cu(111), the FT shown in Fig. 1(b) would have been a *solid disk* of radius  $2k_F$ , *not a ring*.

Referring to the STM experimental observations, the *energy-resolved* charge density (i.e., local density of states) is derived from Eq. (1) and is found to be

$$n_0[E(k), x] \propto \{1 - J_0[2k(E)x]\}. \quad (2)$$

The FT of this equation can be evaluated analytically, yielding an important fact that the intrinsic momentum resolution of the energy-resolved Friedel oscillations is perfect, i.e.,  $\Delta k = 0$ . However, in an actual measurement there is always a finite bias. The low-bias image can be simulated by integrating over the allowed states within the energy window of interest. Since the bias in Fig. 1(a) is 5 mV and the Cu(111) surface-state bandwidth is 400 meV, the result of integrating Eq. (2) over an energy window of the width  $0.1 E_F$  is shown in Fig. 2(a). It is evident that the amplitude of the oscillations is much larger than for the true Friedel oscillations, and, furthermore, the falloff is slower, going as  $1/x^{1/2}$ . To further illustrate the difference, the FT of Eq. (2) is shown as the solid curve in Fig. 2(b), and a single peak at  $q = 2k_F$  is clearly seen. Experimentally, the larger amplitude and the slower falloff of the *energy-resolved* Friedel oscillations, acquired at low-bias voltages, facilitate easier observation of the perturbed charge density in order to extract FC information and circumvent the inherent difficulties of imaging the total charge oscillations using larger bias voltages.<sup>6</sup>

Utilizing this approach, the capabilities of the FT-STM are further illustrated by looking at two different faces of beryllium, whose surface electronic properties resemble true 2D metallic systems due to the low (high) bulk (surface) density of states at  $E_F$ .<sup>10–12</sup> Figures 3(a) and 3(b) show a FT-STM image of the Be(0001) surface at 150 K and the corresponding 2D Brillouin zone indicating the 2D Fermi surface.<sup>12</sup> Due to the short wavelength of the Friedel waves in the present case ( $\lambda_{\text{Be}(0001)} = 3.2 \text{ \AA}$  vs  $\lambda_{\text{Cu}(111)} \approx 15 \text{ \AA}$ ), the circularly centered FC of the surface state extends throughout much of the reciprocal unit cell. As indicated in the figure, the FT-STM image also reveals “spots” corresponding to the reciprocal lattice of the Be(0001) atomic array. This fact allows an internal calibration to a quantitative measurement of the surface wave vector. As in the case of close-

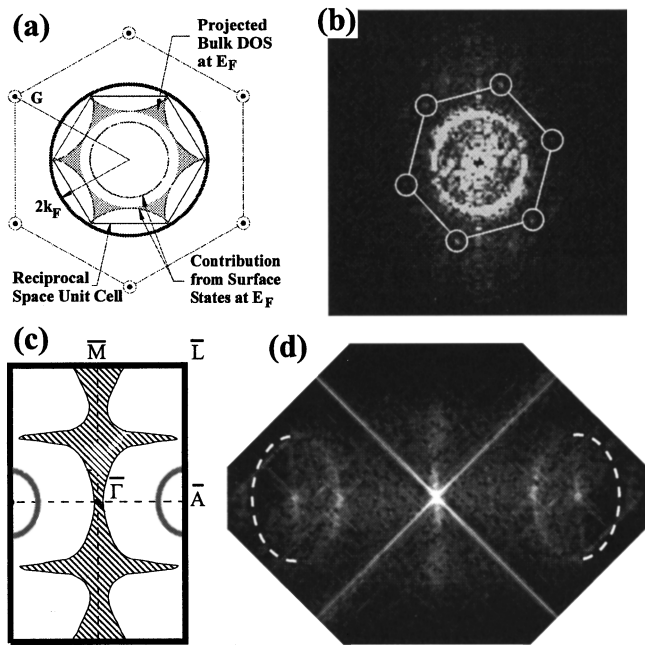


FIG. 3. (a) The 2D Brillouin zone of Be(0001) in which circles (shaded region) correspond to the surface states (bulk projected bands) at  $E_F$ . (b) A FT-STM image of Be(0001) at 150 K (Ref. 12), in which the hexagonal array of “spots” corresponds to the reciprocal lattice. (c) The Be (10 $\bar{1}$ 0) surface Brillouin zone (SBZ) with the calculated surface Fermi contour around  $\bar{A}$  (bulk projected states are crosshatched) (Ref. 20). (d) A FT-STM image of the Be(10 $\bar{1}$ 0) surface. Dotted half ellipses, centered around the  $\bar{A}$  reciprocal lattice spots, have been added to guide the eye [see SBZ in (c)].

packed noble-metal surfaces, the  $k_F$  value determined from FT-STM for Be(0001) compares well with angle-resolved ultraviolet photoemission spectroscopy (ARUPS) results.<sup>13</sup>

Now we want to demonstrate the utility of FT-STM on a system with a decidedly non-free-electron FC, namely, the Be(10 $\bar{1}$ 0) surface whose Fermi contour is non-free electron-like.<sup>10,11</sup> The FC is not a simple ring around the zone center but ellipses centered on the  $\bar{A}$  point at the surface Brillouin-zone boundary [Fig. 3(c)]. As reported by Hofmann *et al.*,<sup>11</sup> the Friedel oscillations observed in STM images of the Be(10 $\bar{1}$ 0) at 4 K reveal a “one-dimensional-like” screening. This is a consequence of the nature of the 2D FC, as is dramatically revealed in the FT-STM image shown in Fig. 3(d). The elliptical Fermi contour, shown Fig. 3(c) is apparent in the image (see dotted lines).

Briner *et al.*<sup>14</sup> have shown that if numerical postprocessing is applied to the STM images of Be(10 $\bar{1}$ 0), higher-order features in FT-STM images are also observed. These correspond to the umklaplike processes with the Bloch waves, that is, momenta features corresponding to wave vectors of  $2k_F \pm nG$ . From these observed characteristics of the higher-order harmonics in the FT-STM images, the wave-function properties of the surface electron state show a significant deviation from plane waves.<sup>14</sup> Although pointed out in the original papers by Ruderman and Kittel<sup>15</sup> and Herman and Schrieffer,<sup>16</sup> the coupling nature of Friedel oscillations with Bloch states has, by and large, been subsequently neglected, but it must play a role in many physical processes (e.g.,

explanation of giant magnetoresistance-type phenomena in layered systems). The ability to observe this type of behavior calls upon new theoretical input to help understand the intensity of the folded-back contours.

The FT-STM measured eccentricity of the Be(10 $\bar{1}$ 0) electron pocket is 0.69,<sup>11</sup> in good agreement with theory (i.e., 0.67) but quite different from photoemission results (i.e., 0.75).<sup>10</sup> Most likely, the reason the FT-STM crossings appear to be closer to theoretical first-principles calculations is due to the difficulty of separating the surface-state emission from the bulk band emission in the ARUPS experiment. As mentioned previously, due to the dimensionality dependent falloff of the wave amplitude, the FT-STM method provides a natural surface sensitivity and a discrimination against bulk band structure artifacts compared to the ARUPS technique.

Because the FT-STM technique seemingly provides the same information that standard ARPES provides, it is important to point out the differences and similarities between these two techniques. A prominent difference between the two techniques is that in STM, a real-space and a reciprocal space image of a very small, selected surface area are produced simultaneously, while ARPES gives only information about the electronic structure integrated over a large area. On samples that are far from perfect, this fact allows one to “preselect” the nanoregion in which the 2D FC is to be determined. A second, significant difference is that in a STM experiment the voltage bias can be either positive or negative, which means that it is equally easy to probe the energy contour above and below the Fermi surface. This can be accomplished by recording a spatial image in a  $dI/dV$  mode<sup>7,8</sup> as a function of  $V$  and Fourier transforming the image. Finally, the time necessary to extract a given 2D FC with FT-STM is considerably less than with the ARPES technique, namely, transforming a single STM image vs acquiring spectra taken throughout many  $k$  points of the surface Brillouin zone.

The key ingredient for any spectroscopic study of the Fermi contour is resolution, both in energy and momentum. The inherent resolution of FT-STM is excellent and, provided that the instrument is operated at low temperature, is potentially superior to the highest-resolution beam lines at third-generation synchrotron radiation sources. The temperature and the bias voltage determine the energy resolution. It is quite easy to operate with mV biases so the inherent limit is  $kT$ , i.e., the tunneling current dependence of the Fermi distribution<sup>8</sup> (a 4 K STM operating in a thermal voltage bias mode  $\sim \mu V$ ,<sup>17</sup> is ideally suited to meet these criteria). Figure 2(b) shows that the inherent momentum resolution is also related to the bias voltage. Since  $E$  and  $k$  are simply related for an effective-mass band, the momentum broadening due to a spread in energy is given by  $\Delta q/q = \Delta k/k = \Delta E/2E$ . Thus the inherent momentum resolution for the Cu(111) image shown in Fig. 1 is  $\Delta k = 0.0004 \text{ \AA}^{-1}$ . However, the measured width of the  $2k_F$  “ring” is  $\sim 0.02 \text{ \AA}^{-1}$ . This is due to the fact that the momentum resolution is dictated by extrinsic factors such as the size of the image, the thermal decay of the standing waves, and the stability of the microscope. First, because of the finite image size it is necessary to perform a discrete FT, which leads to a lower limit for the momentum resolution, since  $\Delta k \propto (\text{image length})^{-1}$ . Second, phenomena that cause a decay of the waves naturally invoke more

Fourier components, leading to a broadening of the Fermi contour. Primary modes of decay include phonon-assisted scattering of the surface-state electrons into bulk states, which increases with temperature, and the Fermi distribution smearing at higher temperatures. Acknowledging these factors, the measured momentum resolution ( $\Delta k/k_F$ ) from FT-STM images [ $\sim 0.12$ , Au(111);  $\sim 0.15$ , Be(0001)] compares well with high-resolution ARPES results [ $0.13$ , Au(111);  $0.05$ , Be(0001)].<sup>13</sup>

As stated previously, the Fermi-level crossings determined from FT-STM are, by and large, comparable with ARUPS results. However, it should be noted that there may be inherent differences between the values determined from these two techniques. The Fermi-line determination in FT-STM relies on the Friedel oscillation near steps and defects. Although these oscillations are the response of the *otherwise unperturbed* electron gas to an impurity, this might only be true to first order and the defect itself may change the electronic structure in its vicinity. Moreover, the physical process of ARPES and STM is not the same. An ARPES experiment corresponds to a sudden emission of an electron (e.g., 10–100 eV) from the sample, while it is taken away adiabatically in STM (e.g.,  $\sim 1$  meV). This might lead to a measurable difference between the two techniques caused by electron-hole and phonon-hole relaxation contribution. In particular, the coupling to the lattice vibrations could be quite different between the two techniques. Moreover, because Friedel oscillations primarily are due to the response of the surface nearly free-electron states, there is a preferential

discrimination against localized states, that is, the 2D FC determined from the FT-STM method may be dictated by parts of the FC with large  $s$  and  $p$  character.

In conclusion, we have presented a powerful technique for the determination of two-dimensional surface Fermi contour. The Fourier transformation of images possessing Friedel oscillations represents a direct image of the 2D Fermi contour. It is proposed that this technique will be widely and generally applicable to a variety of other material surfaces to extract 2D Fermiology related information on a nanometer scale. This includes high- $T_c$  materials (e.g., measurement of van Hove singularities near the Fermi energy), magnetic materials (e.g., elucidation of spin-density wave “shadow bands” arising from quasielastic exchange Bragg scattering<sup>18</sup>), and surface chemistry (e.g., long-range ordering and interaction of chemisorbed atoms/molecules). Since what is measured with FT-STM is directly related to the 2D response function, many-body effects can be directly probed.<sup>15,19</sup>

This work was supported by the National Science Foundation under Grant No. NSF-95-10132, by CAMP (Center for Atomic-scale Materials Physics) sponsored by the Danish National Research Foundation, by the VELUX Foundation, and by the Knud Højgaard Foundation. Ph. Hofmann thanks the Alexander v. Humboldt-Stiftung for financial support. Part of this study was conducted at ORNL and supported by the U.S. Department of Energy under Contract No. DE-AC05-96OR22464 with Lockheed Martin Energy Research Corp.

\*Present address: Fritz-Haber-Institut der Max-Planck-Gesellschaft, Berlin, Germany.

<sup>1</sup>G. Grüner, *Density Waves in Solids* (Addison-Wesley, Reading, MA, 1994).

<sup>2</sup>S. D. Kevan, *Phys. Scr.* **T31**, 32 (1990); *Surf. Sci.* **307**, 832 (1994).

<sup>3</sup>W. E. Pickett, H. Krakauer, R. E. Cohen, and D. J. Singh, *Science* **255**, 46 (1992).

<sup>4</sup>J. Friedel, *Nuovo Cimento Suppl.* **7**, 287 (1958).

<sup>5</sup>J. Tersoff and D. R. Hamann, *Phys. Rev. B* **31**, 805 (1985).

<sup>6</sup>G. Hörmandinger, *Phys. Rev. B* **49**, 13 897 (1994).

<sup>7</sup>M. F. Crommie, C. P. Lutz, and D. M. Eigler, *Nature (London)* **363**, 524 (1993); E. J. Heller, M. F. Crommie, C. P. Lutz, and D. M. Eigler, *ibid.* **369**, 464 (1994).

<sup>8</sup>Y. Hasegawa and Ph. Avouris, *Phys. Rev. Lett.* **71**, 1071 (1993); Ph. Avouris, I.-W. Lyo, R. E. Walkup, and Y. Hasegawa, *J. Vac. Sci. Technol. B* **12**, 1447 (1994).

<sup>9</sup>S. D. Kevan and R. H. Gaylord, *Phys. Rev. B* **36**, 5809 (1987).

<sup>10</sup>Ph. Hofmann, R. Stumpf, V. M. Silkin, E. V. Chulkov, and E. W. Plummer, *Surf. Sci.* **355**, L278 (1996).

<sup>11</sup>Ph. Hofmann, B. G. Briner, M. Doering, H.-P. Rust, E. W. Plummer, and A. M. Bradshaw, *Phys. Rev. Lett.* **79**, 265 (1997).

<sup>12</sup>P. T. Sprunger, L. Petersen, E. W. Plummer, E. Lægsgaard, and F. Besenbacher, *Science* **275**, 1764 (1997).

<sup>13</sup>E. Jensen (private communication).

<sup>14</sup>B. G. Briner, Ph. Hofmann, M. Doering, H.-P. Rust, E. W. Plummer, and A. M. Bradshaw, *Europhys. Lett.* **39**, 67 (1997).

<sup>15</sup>M. A. Ruderman and C. Kittel, *Phys. Rev.* **96**, 99 (1954).

<sup>16</sup>F. Herman and J. R. Schrieffer, *Phys. Rev. B* **46**, 5806 (1992).

<sup>17</sup>D. Hoffman, A. Haas, T. Kunstmann, J. Seifritz, and R. Möller, *J. Vac. Sci. Technol. A* **15**, 1418 (1997).

<sup>18</sup>J. R. Schrieffer and A. P. Kampf, *J. Phys. Chem. Solids* **56**, 1673 (1995).

<sup>19</sup>P. F. Maldague, *Surf. Sci.* **73**, 296 (1978).